

MicroRNA-23a/b and microRNA-27a/b suppress Apaf-1 protein and alleviate hypoxia-induced neuronal apoptosis

Q Chen¹, J Xu¹, L Li¹, H Li¹, S Mao¹, F Zhang¹, K Zen^{*1}, C-Y Zhang^{*1} and Q Zhang^{*1}

Expression of apoptotic protease activating factor-1 (Apaf-1) gradually decreases during brain development, and this decrease is likely responsible for the decreased sensitivity of brain tissue to apoptosis. However, the mechanism by which Apaf-1 expression is decreased remains elusive. In the present study, we found that four microRNAs (miR-23a/b and miR-27a/b) of miR-23a-27a-24 and miR-23b-27b-24 clusters play key roles in modulating the expression of Apaf-1. First, we found that miR-23a/b and miR-27a/b suppressed the expression of Apaf-1 *in vitro*. Interestingly, the expression of the miR-23-27-24 clusters in the mouse cortex gradually increased in a manner that was inversely correlated with the pattern of Apaf-1 expression. Second, hypoxic injuries during fetal distress caused reduced expression of the miR-23b and miR-27b that was inversely correlated with an elevation of Apaf-1 expression during neuronal apoptosis. Third, we made neuronal-specific transgenic mice and found that overexpressing the miR-23b and miR-27b in mouse neurons inhibited the neuronal apoptosis induced by intrauterine hypoxia. In conclusion, our results demonstrate, in central neural system, that miR-23a/b and miR-27a/b are endogenous inhibitory factors of Apaf-1 expression and regulate the sensitivity of neurons to apoptosis. Our findings may also have implications for the potential target role of microRNAs in the treatment of neuronal apoptosis-related diseases.

Cell Death and Disease (2014) 5, e1132; doi:10.1038/cddis.2014.92; published online 20 March 2014

Subject Category: Neuroscience

Apoptosis occurs throughout the nervous system during development. It is estimated that at least half of the original cellular population is eliminated as a result of apoptosis in the developing nervous system because of the processes of the optimization of synaptic connections and removal of unnecessary neurons as well as pattern formation.¹ Deletion of apoptotic genes from early development is lethal to the embryo.^{2–4} Interestingly, despite the ubiquitous expression of caspase-3 and caspase-9 throughout the organs of the body, the main pathology that arises from a deficiency in apoptosis is focused on the developing brain that reveals the essential physiological role of apoptosis in neural development. Pathologically, apoptosis and dysregulation of apoptosis also play roles in nervous system diseases, for example, infectious, degenerative, and neoplastic diseases of the nervous system.⁵ Among the multiple etiologies of perinatal brain injuries, hypoxia–ischemia is the most common and predominant.⁶ Hypoxia–ischemia is thought to be the final common end point for a complex convergence of events; some of these events are genetically determined and some are triggered by an *in utero* (but not necessarily intrapartum) stressor.⁷ Although apoptosis occurs after hypoxia–ischemia

in both embryonic and adult stages, multiple studies have suggested that apoptosis plays a more prominent role in the embryo than in the adult after brain injuries caused by hypoxia–ischemia.^{8–10} This differential sensitivity of the brain to apoptosis may be explained, in part, by the differential age-dependent expression of apoptotic genes, mainly the apoptotic protease activating factor-1 (*Apaf-1*) gene.¹¹

Apaf-1 is a component protein of the apoptosome. In the intrinsic apoptosis pathway, cytochrome *c* is released from the mitochondria to the cytosol and binds to Apaf-1 protein. Binding of cytochrome *c* to Apaf-1 allows the recruitment and activation of caspase-9 within the apoptosome.¹² Deficiency in Apaf-1 is lethal to mouse embryos. Homozygous mutants die at embryonic day 16.5, and their phenotype includes severe craniofacial malformations, brain overgrowth, persistence of the interdigital webs, and dramatic alterations of the lens and retina.¹³ High level of Apaf-1 expression in brain tumors elevates the sensitivity of the brain tumors to apoptosis induced by cytochrome *c* that reveals that the protein level of Apaf-1 may directly influence the sensitivity of brain cells to apoptotic stimuli.¹⁴ Therefore, as a key apoptotic protein that may decide the apoptotic fate of cells, Apaf-1 expression is

¹State Key Laboratory of Pharmaceutical Biotechnology, Jiangsu Engineering Research Center for microRNA Biology and Biotechnology, School of Life Sciences, Nanjing University, Nanjing, Jiangsu, China

*Corresponding authors: Q Zhang or C-Y Zhang or K Zen, State Key Laboratory of Pharmaceutical Biotechnology, Jiangsu Engineering Research Center for microRNA Biology and Biotechnology, School of Life Sciences, Nanjing University, Nanjing University, 22 Hankou Road, Nanjing, Jiangsu 210093, China. Tel/Fax: +86 25 84530990; E-mail: qzhang@nju.edu.cn (QZ) or Tel/Fax: +86 25 83686234; E-mail: cyzhang@nju.edu.cn (C-YZ) or Tel/fax: +86 25 84530231; E-mail: kzen@nju.edu.cn (KZ)

Keywords: brain development; neuron; apoptosis; microRNA; fetal distress

Abbreviations: Apaf-1, apoptotic protease activating factor-1; IHC, immunohistochemistry; miRNA, microRNA; Tubb3, tubulin β III; TUNEL, terminal deoxynucleotidyl transferase-mediated dUTP-biotin nick end labeling

Received 21.10.13; revised 21.1.14; accepted 10.2.14; Edited by D Bano

tightly regulated. Previous studies have reported that the expression of Apaf-1 decreases in rat cerebral cortex during development, and this would explain the high sensitivity of the nervous system to apoptosis at the embryonic stage. However, the mechanism by which Apaf-1 expression is downregulated in the brain during development is still unknown.

MicroRNAs (miRNAs) are a group of endogenous noncoding RNAs that consist of 18 to 25 nucleotides. The miRNAs play an important role in regulating gene expression at the posttranscriptional level by binding to complementary sites on target mRNAs that either block mRNA translation or trigger mRNA degradation.^{15,16} The diversity of miRNAs and the multiple genes that are targeted by every miRNA provide miRNAs with versatile functions in the control of gene expression.¹⁷ Currently, miRNAs are thought to regulate the expression of most genes and, consequently, play regulatory roles in a wide variety of physiological and pathological cellular processes.¹⁸ In the nervous system, miRNAs have temporally and spatially specific expression patterns during the development of the brain^{19–21} and thus contribute to the processes of determining neuronal cell identities and specific functions.^{22,23} In nervous system diseases, miRNAs may be dysregulated and influence the pathological progress and outcomes. Changes in the miRNA profile of the adult brain during hypoxia–ischemia have been reported. For example, in microglia cells, hypoxia causes the upregulation of FasL expression and the downregulation of miR-21 expression during hypoxia-induced microglial activation.²⁴ Doeppner *et al.*²⁵ reported that miR-124 promotes neuronal survival under ischemic conditions via Usp14-dependent REST degradation. However, the alterations in miRNAs during perinatal hypoxic–ischemic encephalopathy are still largely unknown.

In the present study, we tested the hypothesis that miRNAs may regulate Apaf-1 expression in the mouse cortex during development and in neurological diseases. We found miR-23a/b and miR-27a/b encoded by the miR-23a-27a-24 and miR-23b-27b-24 clusters that participated in the regulation of Apaf-1 expression. With various methods, we showed that the expression of miR-23-27-24 clusters gradually increased in the mouse cortex in a manner that was inversely correlated with the pattern of Apaf-1 expression. Furthermore, in a hypoxia-induced neuronal apoptosis mouse model, overexpression of the miR-23b and miR-27b clusters inhibited the neuronal apoptosis induced by intrauterine hypoxia. For the first time, we discovered that miRNAs regulate the sensitivity of neurons to apoptosis during development and hypoxia-induced brain injuries.

Results

Apaf-1 gene expression decreases during development in the mouse cerebral cortex. Previous studies have reported that the expression of Apaf-1 decreases during development in the rat cortex.¹¹ Thus, we initially examined the expression of Apaf-1 protein and mRNA in the mouse cortex during brain development in the present study. Four time points were chosen to represent the entire developmental process: E18, P7, P14, and the adult stage

(P60). We found that the Apaf-1 protein levels decreased as cortical development progressed (Figure 1a). Similarly, Apaf-1 mRNA also decreased during brain development (Figure 1b). Furthermore, immunohistochemistry (IHC) stain showed that the neuronal cells had little signal of Apaf-1 protein in the adult stage, whereas Apaf-1 protein was expressed in the neurons at the E18 stage (Figure 1c). This differential expression of Apaf-1 is consistent with the decreases in susceptibility to apoptosis during mouse brain development that implies that expression of Apaf-1 might contribute to the susceptibility of neurons to apoptosis.

Upregulation of miR-23-27-24 clusters during development in mouse cortex is inversely correlated with the Apaf-1 expression pattern.

Compared with the downregulation of the mRNA level, the decrease of Apaf-1 protein level was more dramatic, and this indicates that Apaf-1 gene expression might be regulated at the posttranscriptional level. The miRNAs are a type of endogenous small RNA that suppresses gene expression at the posttranscriptional level. Using computer-aided algorithms,²⁶ we found that four (miR-23a, miR-23b, miR-27a, and miR-27b) of the miR-23-27-24 clusters had conserved putative binding sites for Apaf-1 mRNA on 3'-UTR (Figure 2a). The miR-24 had less conserved binding sites. In the mouse genome, the mmu-miR-23a-27a-24-2 cluster is located on chromosome 8, and the mmu-miR-23b-27b-24-1 cluster is located on chromosome 13. We examined the levels of miR-23a/b, miR-27a/b, and miR-24 expression at the same developmental time points. The results from quantitative reverse transcription-PCR (qRT-PCR) experiments showed that expression of the miR-23-27-24 clusters clearly increased over these time points. The miR-23b expression gradually increased during maturation of the brain, and the miR-23b transcript levels were approximately fivefold greater in adult mouse cortices than in the cortices of the E18 pups. The miR-27b also exhibited dramatically increased expression in the adult stage. The miR-23a and miR-27a also showed gradually increases in expression, but these increases were relatively mild compared with that of the miR-23b-27b cluster. The miR-24 had a significantly increased expression pattern during development (Figure 2b). To further corroborate the qRT-PCR results, a RNA dot blotting assay and *in situ* hybridization staining were employed. As shown in Figure 2c, miR-23b levels were much higher in P60 adult mouse cortices than in E18 pup cortices. In contrast to IHC staining signal of Apaf-1, the *in situ* hybridization results revealed that miR-23b was abundantly expressed in the neurons and more miR-23b signals were detected in adult brain neurons (Figure 2d). Therefore, the expression patterns of the Apaf-1 gene and the miR-23-27 clusters were inversely correlated that indicates that the miR-23-27 clusters might inhibit Apaf-1 gene expression during brain development.

MiR-23a/b and miR-27a/b suppress Apaf-1 expression at the posttranscriptional level. Gene expression analysis showed that the expression patterns of the miR-23-27-24 clusters were inversely correlated with that of the Apaf-1 gene. To confirm that these miRNAs actually suppress Apaf-1 gene expression, we performed the following studies.

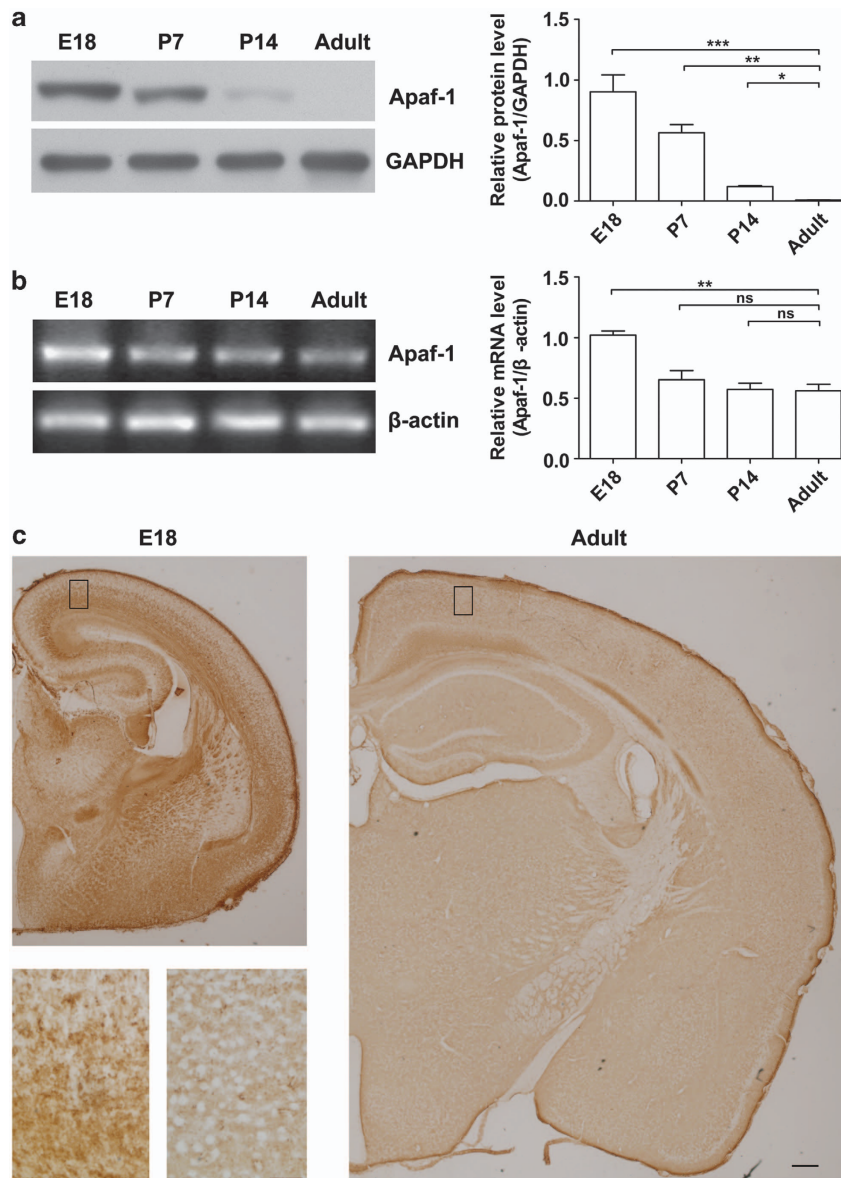


Figure 1 Decreased Apaf-1 gene expression during brain development. (a) Representative western blots of Apaf-1 in cortical samples at different developmental stages (E18, P7, P14, and adult). Each lane was loaded with equal amounts of total protein from the mixed samples of five individuals ($n = 5$, unpaired t -test, $*P < 0.05$, $**P < 0.01$, and $***P < 0.001$). (b) Semiquantitative RT-PCR detection of Apaf-1 mRNA in the total RNA from cerebral cortices at different developmental stages. Quantitative RT-PCR detection of Apaf-1 mRNA ($n = 5$, unpaired t -test, NS, not significant, $**P < 0.01$). Error bars represent the S.E.M. (c) IHC stain of Apaf-1 in E18 and adult brain tissues. Scale bar represents $250 \mu\text{m}$; scale bar (insert) represents $50 \mu\text{m}$

A 507-bp-length DNA that contains the putative binding sites for miR-23a/b, miR-27a/b, and miR-24 was cloned from the 3'-UTR of Apaf-1 mRNA to the pMIR-REPORT Luciferase plasmid. Then, luciferase assays were performed in HEK293T cells. Overexpression of miR-23a/b or miR-27a/b significantly suppressed luciferase activity. Conversely, after introducing mutations to seven sites in the predicted miRNA binding site on 3'-UTR of the plasmid, the inhibitory effect of overexpression of miR-23a/b or miR-27a/b was abolished (Figure 3a). However, overexpression of miR-24 had little effect on luciferase activity (Supplementary Figure 1a). Furthermore, western blotting analyses showed that Apaf-1 protein levels were decreased after cells received miR-23a/b or miR-27a/b (Figure 3b). Overexpression of miR-24 had little

effect on Apaf-1 expression (Supplementary Figure 1b). These results indicate that miR-23a/b and miR-27a/b of miR-23-27-24 clusters suppressed Apaf-1 gene expression.

Hypoxia causes increased neuronal apoptosis and increased Apaf-1 protein expression. Physiologically, sporadic apoptotic cell death provides a selective mechanism that removes surplus or unwanted neurons during the process of brain development. However, apoptosis is uncommon in the mature mammalian brains under normal physiological conditions.²⁷ Neuronal apoptosis also occurs in cortical neurons in many pathological conditions. Reduced oxygen supply (hypoxia) during the pre- and perinatal periods often leads to neonatal brain damage. Indeed, perinatal

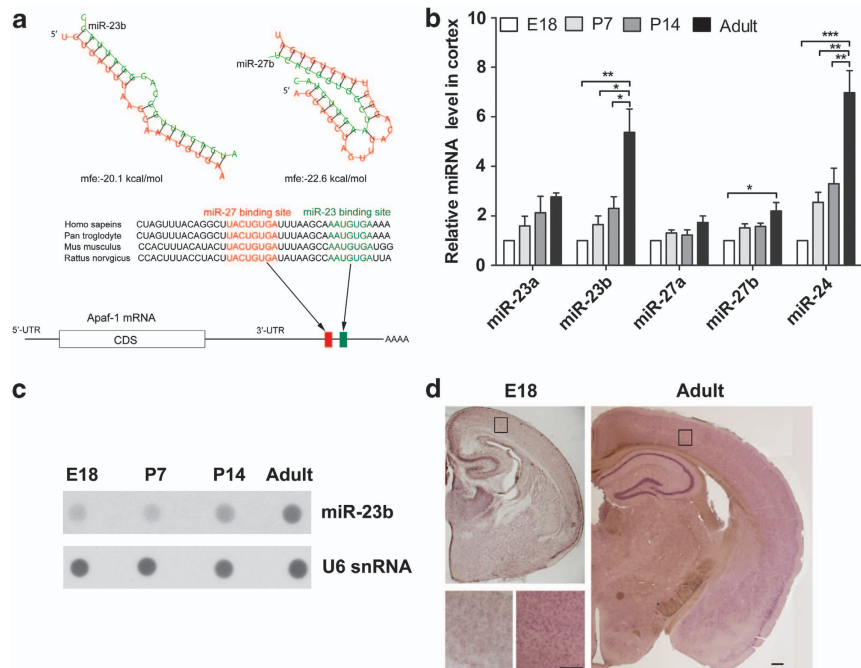


Figure 2 The expression of miR-23-27 clusters increases during brain development. (a) Schematic of the Apaf-1 3'UTR indicating the locations of the miR-23 and miR-27 target sites that are conserved in vertebrates. The Apaf-1 3'UTR contains evolutionarily well-conserved sequences matched for the miR-23 and miR-27 families that were predicted by computer-aided algorithms. The free energies (mfes) of microRNA bindings were calculated by RNAHybrid software (BiBiServ, Bielefeld, Germany). (b) Quantitative RT-PCR detection of miR-23a, miR-23b, miR-27a, miR-27b, and miR-24 in cerebral cortex samples at different developmental stages ($n=5$, one-way ANOVA with Newman–Keuls multiple comparison test, * $P < 0.05$, ** $P < 0.01$, and *** $P < 0.001$). (c) Dot blot analyses of miR-23b and U6 snRNA in total RNA of the cerebral cortex. Each lane was loaded with equal amounts of total RNA extracted from the mixed samples of five individuals. (d) Expression of miR-23b in cortices of E18 and adult brain tissues detected by *in situ* hybridization. Scale bar represents 250 μm ; scale bar (insert) represents 200 μm

hypoxic–ischemic encephalopathy is a significant cause of mortality and morbidity in infants and young children, and apoptosis is thought to play an important role in perinatal hypoxic–ischemic encephalopathy.²⁸ In a fetal distress mouse model, we observed a dramatic increase in apoptotic neurons in the E19.5 pup cortex exposure to hypoxia (Figure 4a). We examined whether Apaf-1 protein levels changed in hypoxia-treated cortices. As shown in Figure 4b, the expression of Apaf-1 protein was significantly increased at 12 and 24 h after 6 h of hypoxia treatment. Meanwhile, the expression of the miR-23b and miR-27b decreased before alterations in Apaf-1 expression at the 6-h time point after hypoxia treatment (Figure 4c). In primary cortical neurons, anaerobic treatment also caused increases in Apaf-1 protein expression and decreases in miR-23b and miR-27b expression (Figures 4d and e). These results imply that miR-23b and miR-27b are downregulated during hypoxia that relieves the miRNA-mediated inhibition of Apaf-1 expression and increases the sensitivities of neurons to apoptosis.

Overexpression of the miR-23b and miR-27b attenuates neuronal apoptosis through suppression of Apaf-1. We investigated the role of Apaf-1 in neuronal apoptosis induced by hypoxia. A specific siRNA of Apaf-1 was employed to knock down Apaf-1 expression (Figure 5a). After the primary cortical neurons received the siRNA, these neurons received an anaerobic treatment (24 h), as we found that the cultured neurons were resistant to hypoxia treatment *in vitro*. We found that the neuronal apoptosis rate, calculated by cleaved

caspase-3-positive neurons or terminal deoxynucleotidyl transferase-mediated dUTP-biotin nick end labeling (TUNEL) staining positive neurons respectively, was significantly decreased in siRNA group (Figure 5b). To examine the effects of miR-23b and miR-27b on hypoxia-induced neuronal apoptosis, we overexpressed miR-23b or miR-27b in primary cortical neurons, and these neurons received the anaerobic treatment (24 h). Western blot analyses showed that miR-23b or miR-27b significantly downregulated Apaf-1 protein levels (Figure 5c). Furthermore, the numbers of apoptotic neurons were reduced after the overexpression of miR-23b or miR-27b (Figure 5d). Next, we put an Apaf-1 expression vector into the neurons to elevate the Apaf-1 expression level that had received miR-23b or miR-27b precursor miRNAs to decrease Apaf-1 expression (Figure 6a). As shown in Figures 6b and c, elevated Apaf-1 expression caused a significant increase of neuronal death during hypoxia, and even miR-23b or miR-27b was also overexpressing. These results indicate that Apaf-1 is the main target of miR-23 and miR-27 during hypoxia, and through suppressing Apaf-1, miR-23a/b and miR-27a/b regulate the sensitivity of neuron to apoptosis.

To further confirm the roles of miR-23b and miR-27b in neuronal apoptosis, we constructed neuronal-specific miR-23b-27b cluster transgenic mice. In these transgenic mice, the promoter of the *tubulin β III* (*Tubb3*) gene was employed because of its high expression capability in the early embryonic brain stage (E9.5)²⁹ that should allow for the ectopic overexpression of the miR-23b-27b cluster in

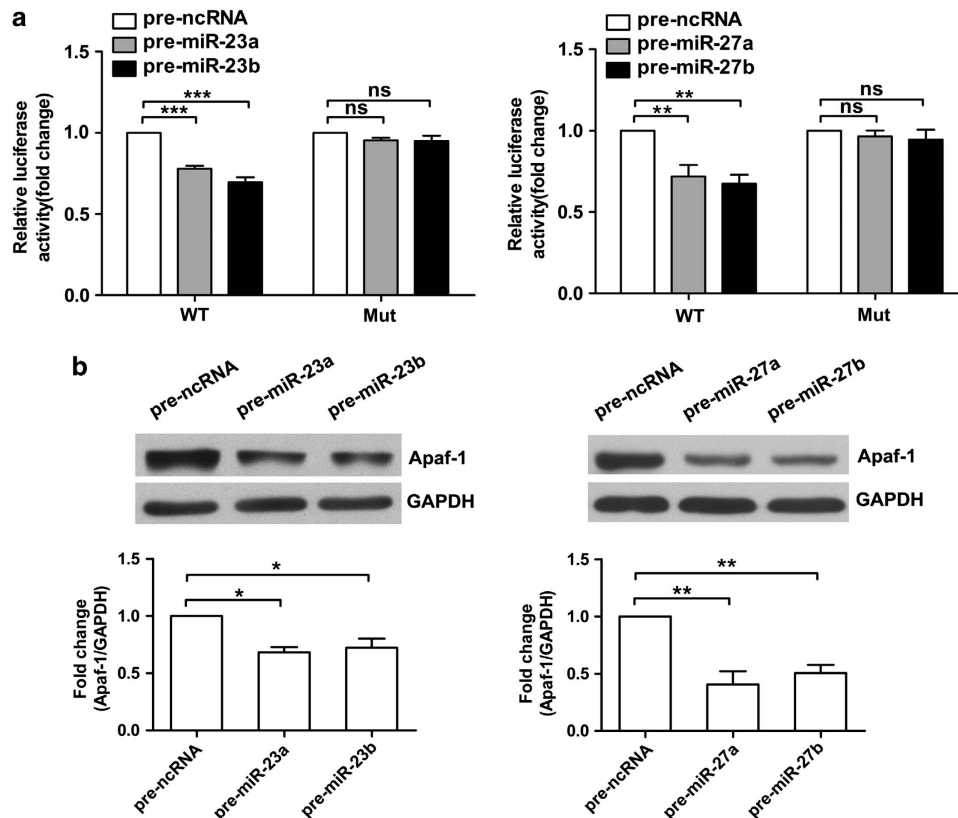


Figure 3 The miR-23a/b and miR-27a/b suppress Apaf-1 protein expression. (a) HEK-293T cells were transfected with luciferase reporter plasmids carrying wild-type (WT) or mutant (Mut) Apaf-1 3'-UTRs. The luciferase activities were examined in the presence of pre-miR-23a/b (left) or pre-miR-27a/b (right) ($n = 5$, unpaired *t*-test, NS, not significant, $**P < 0.01$ and $***P < 0.001$). (b) Apaf-1 protein level in HEK-293T cells 48 h after transfection with pre-miR-23a/b or pre-miR-27a/b ($n = 5$, unpaired *t*-test, $*P < 0.05$ and $**P < 0.01$)

developing cortices. The efficiency of the *Tubb3* promoter was tested in primary neurons; miR-23b expression was ~20-fold greater, and miR-27b expression was ~10-fold greater after transfection of the miR-23b-27b expression plasmid (Figure 7a). Among the 10 founder transgenic mouse lines that were established (Supplementary Figure 2), we chose the line with the highest expression (the B line) and the respective wild-type (WT) mice as controls for further study. We found that the expression of miR-23b and miR-27b were significantly elevated in the transgenic mouse primary neuron cultures, and the expression of the Apaf-1 protein in transgenic mouse primary neurons was decreased (Figure 7b). Immunofluorescent staining of cleaved caspase-3 showed that the apoptotic rate was lower in transgenic mouse primary neurons than in WT mouse primary neurons (Figure 7c) after anaerobic treatment for 24 h. Similarly, TUNEL staining showed that the apoptotic rate was significantly lower in transgenic mouse primary neurons (Figure 7d). We further examined the expression levels of miR-23b and miR-27b in transgenic E19.5 mouse cortices. The miR-23b levels were elevated by ~1.5-fold, and miR-27b levels were elevated by ~2.5-fold in these transgenic mice. Consistently, the expression of Apaf-1 was reduced in the cortices of these mice (Figure 7e). After hypoxia treatment, the numbers of cleaved caspase-3-positive apoptotic neurons were reduced in the cortices of transgenic E19.5 pups. Similarly, TUNEL staining revealed that there were fewer

apoptotic cells in the brains of miR-23b-27b transgenic mice (Figure 7f). Together, these results indicate that overexpression of the miR-23b-27b cluster alleviates neuronal apoptosis by inhibiting Apaf-1 in hypoxia-induced pathological conditions.

Discussion

Apaf-1 is believed to be a key functional protein in physiological apoptosis during brain development and in pathological apoptosis related to CNS injury.¹¹ In the present study, we found that the expressions of miR-23-27-24 clusters were elevated during brain maturation in a manner that was inversely correlated with Apaf-1 expression. The miR-23a/b and miR-27a/b could suppress Apaf-1 expression. Furthermore, the expression of the miR-23-27-24 was down-regulated in brain tissue in a fetal distress mouse model. Forced expression of the miR-23b and miR-27b clusters suppressed Apaf-1 and alleviated neuronal apoptosis in primary cultured neurons and in E19.5 pup cortical neurons after hypoxia. These results show that miRNAs participate in the regulation of Apaf-1 gene expression and play important roles in physiological apoptosis during brain development and in pathological apoptotic processes caused by hypoxia.

The miRNAs modulate complex physiological and pathological processes by repressing the expression of multiple proteins. These inhibitory roles of miRNAs on gene expression are mediated by the imperfect base-match-guided

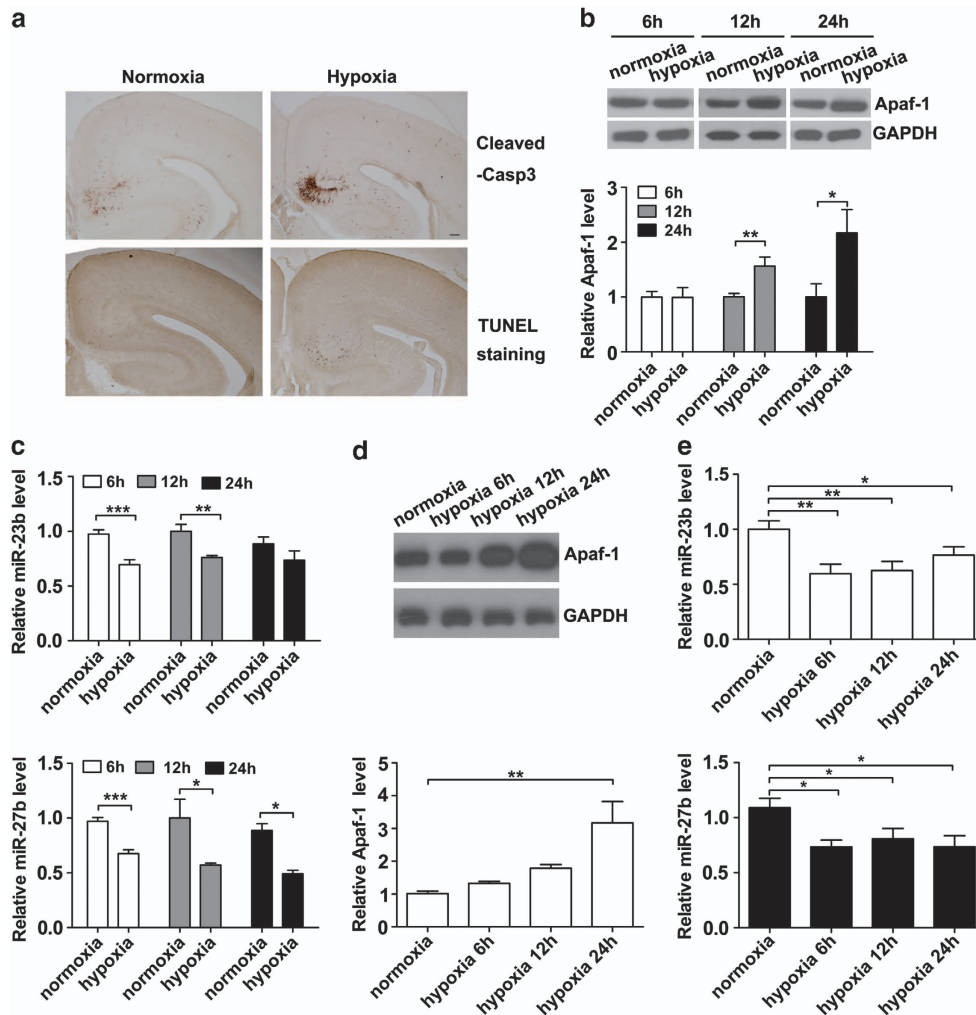


Figure 4 Apaf-1 protein levels are elevated and miR-23b-27b cluster is decreased in cortices of E19.5 pups after hypoxia. (a) Coronal brain sections of E19.5 mice were stained with a cleaved caspase-3 (Cleaved-Casp3) antibody or with TUNEL staining kit. More positively stained neurons were observed in the hypoxia group ($n = 3$) compared with the normoxia control group ($n = 3$). Scale bar represents $100 \mu\text{m}$. (b) Representative western blot images for Apaf-1 in the cerebral cortex under conditions of normoxia or hypoxia for 6 h followed by different recovery times (no recovery, recovery 6 h, or recovery 18 h). Relative fold changes of Apaf-1 protein level were quantified by densitometry ($n = 5$, unpaired t -test, $*P < 0.05$ and $**P < 0.01$). (c) Quantitative RT-PCR detection of miR-23b and miR-27b expression in the cerebral cortices of different groups ($n = 5$, unpaired t -test, $*P < 0.05$, $**P < 0.01$, and $***P < 0.001$). (d) Representative western blot images for Apaf-1 in primary cortical neurons under conditions of normoxia or hypoxia for 6, 12, and 24 h ($n = 3$, unpaired t -test, $**P < 0.01$). (e) Quantitative RT-PCR detection of miR-23b and miR-27b expression in primary cortical neurons under the conditions of normoxia or hypoxia for 6, 12, and 24 h ($n = 6$, unpaired t -test, $*P < 0.05$ and $**P < 0.01$)

binding of miRNAs to their target mRNAs, and it is this imprecise binding that allows each miRNA to target multiple mRNAs. Moreover, different miRNA binding sites may exist on the mRNA of a single gene. The miRNAs may act synergistically in cells of the tissue to enhance their suppressive effects on their common target genes; miRNAs can also function independently in the cells of different tissues. This versatile characteristic of miRNAs broadly extends the regulatory roles of miRNAs. We found that mmu-miR-23a/b and mmu-miR-27a/b had experimentally validated binding sites on the 3'-UTR of Apaf-1 mRNA, but not miR-24. In humans, hsa-miR-23a/b and hsa-miR-27a/b are predicted to be highest possible miRNAs that regulate Apaf-1 expression (miRanda-mirSVR and Targetscan). Very recently, Lian *et al.*³⁰ have reported that the expression of miR-23a in human glioma tissues is significantly upregulated.

Furthermore, they analyzed the results by using the luciferase reporter assay and western blot analysis in 293T cells and glioma cell line, respectively. This finding confirms that hsa-miR-23 suppresses human Apaf-1 expression. We found that the expression of each miRNA of miR-23-27-24 clusters increased during brain development, whereas the expression of Apaf-1 decreased during development. The inversely correlated expression patterns of Apaf-1 and the miR-23-27-24 clusters indicate that the miR-23a/b and miR-27a/b clusters function synergistically to repress Apaf-1 protein during the physiological development process.

Interestingly, according to the predictions of the miRanda-mirSVR algorithm,³¹ miR-23a/b also have putative binding sites for the human caspase-3 gene. Thus, the miR-23a/b and miR-27a/b may suppress multiple key proteins in the apoptosis pathway in human brain development.

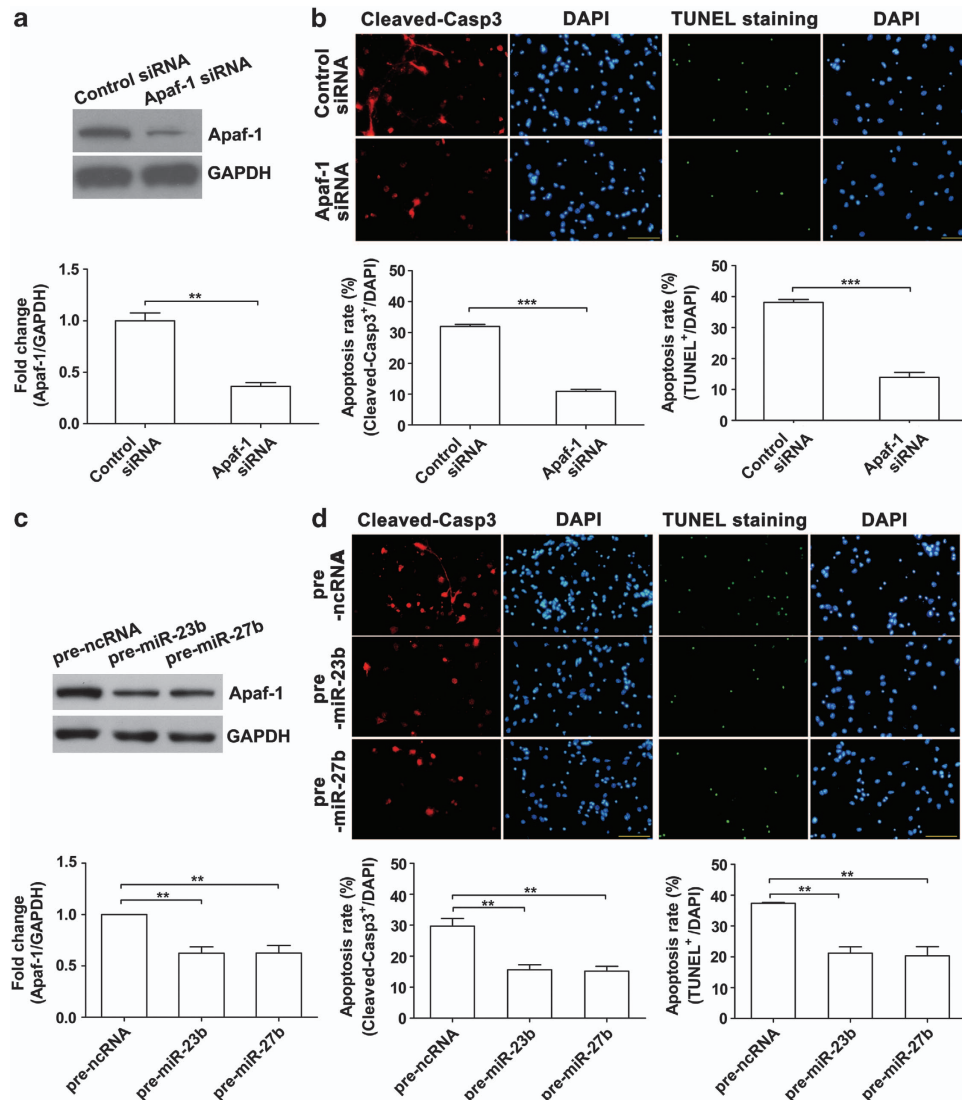


Figure 5 Overexpression of miR-23b or miR-27b represses Apaf-1 protein levels in primary cortical neurons and attenuates neuronal apoptosis caused by hypoxia. (a) Western blot analysis of Apaf-1 in primary cortical neurons 48 h after transfection with Apaf-1 siRNA. Relative amounts of Apaf-1 protein were quantified by densitometry ($n=3$, unpaired t -test, $**P<0.01$). (b) Immunofluorescence staining of Cleaved-Casp3 or TUNEL staining. Neurons were stained with Cleaved-Casp3 antibody or with TUNEL stain kit after hypoxia treatment (24 h) at DIV5. Statistical analysis of the percentage of Cleaved-Casp3-positive neurons or TUNEL-positive neurons to DAPI-stained cells (cell numbers = 400–500, unpaired t -test, $***P<0.001$). (c) Western blot analysis of Apaf-1 in primary cortical neurons 48 h after transfection with pre-miR-23b or pre-miR-27b. Relative amounts of Apaf-1 protein were quantified by densitometry ($n=3$, unpaired t -test, $**P<0.01$). (d) Immunofluorescence staining of Cleaved-Casp3 or TUNEL staining (cell numbers = 600–700, unpaired t -test, $**P<0.01$). Scale bar represents 100 μm

Moreover, it is likely that other miRNAs also synergistically suppress Apaf-1 and other proteins involved in apoptotic pathways.

Previous studies have noted that the sensitivity of the central nervous system to apoptosis is highest at the embryonic stage and gradually decreases during development. Physiologically, apoptosis is designed to remove unnecessary or unsuitable nerve cells that are overproduced during development. However, elevated sensitivity to apoptosis is a double-edged sword because embryonic neuronal cells are highly sensitive to various pathological injuries. Apoptosis may be the major pathway of cell death during the embryonic stage, and pathological neuronal apoptosis is more evident during the embryonic stage. Multiple studies

have suggested that the role of neuronal apoptosis after hypoxia–ischemia in the neonate brain is more prominent than in the adult brain in which necrosis seems to be more prominent.^{7–10} Inhibition of Apaf-1 signaling pathway can confer neuroprotection in rodent models of neonatal hypoxia–ischemia.³² The early forced expression of miR-23b–27b in transgenic mice allowed us to examine the inhibitory roles of miR-23b–27b on neuronal apoptosis induced by hypoxia. Our qRT-PCR results demonstrated that the expression of miR-23b and miR-27b increased significantly in transgenic mice during the embryonic stage. Importantly, the expressions of miR-23b and miR-27b were increased within the physiological range. IHC staining results showed that cleaved caspase-3-positive and TUNEL

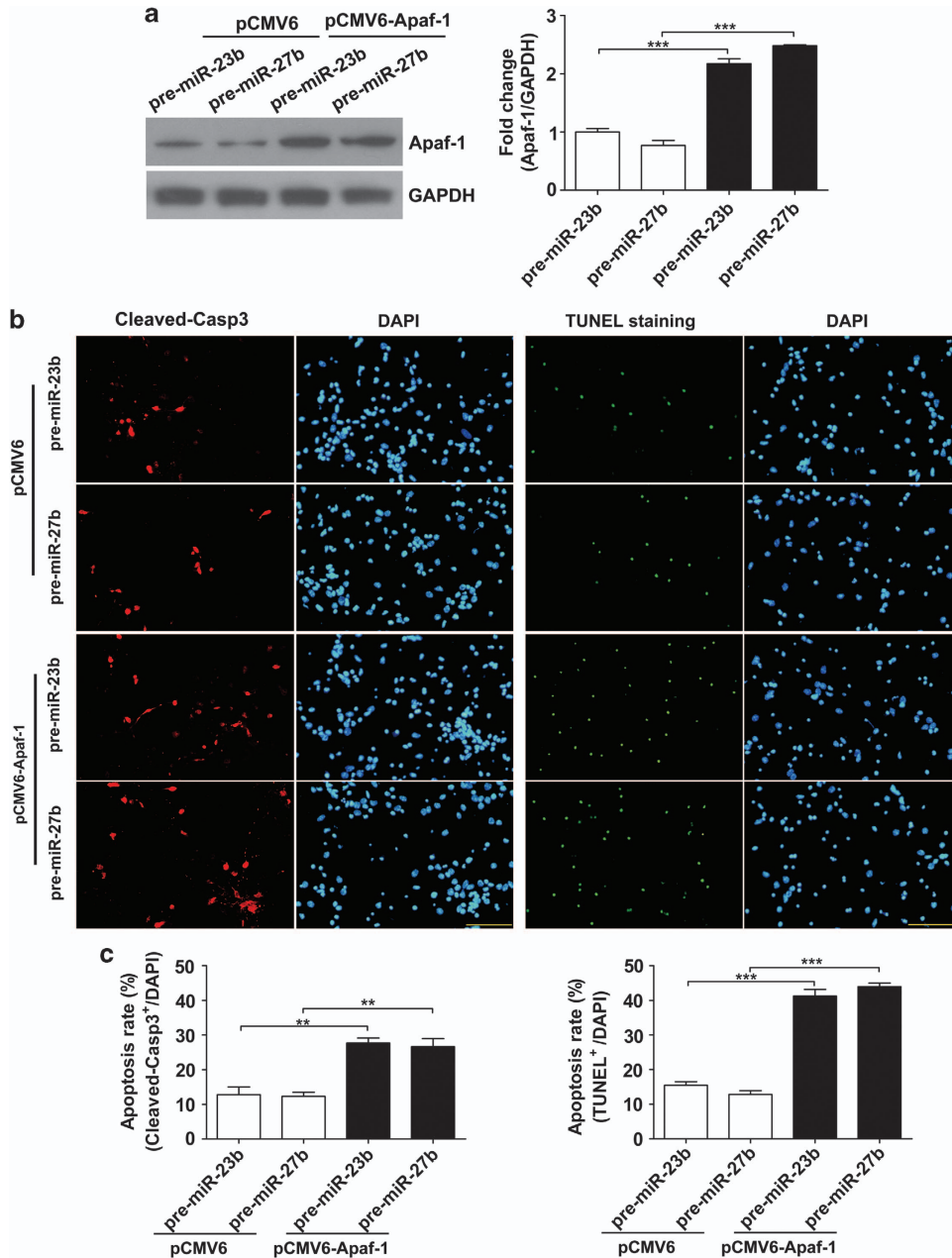


Figure 6 Overexpression of Apaf-1 re-activates the sensitivity of neurons overexpressing miR-23b/27b to apoptosis induced by hypoxia. (a) Western blot analysis of Apaf-1 in primary cortical neurons 48 h after co-transfection with plasmids (pCMV6 or pCMV6-Apaf-1) and miRNAs (pre-miR-23b or pre-miR-27b). Relative amounts of Apaf-1 protein were quantified by densitometry ($n=3$, unpaired t -test, $***P<0.001$). (b) Immunofluorescence staining of Cleaved-Casp3 or TUNEL staining. Cultured cortical neurons co-transfected with plasmids (pCMV6 or pCMV6-Apaf-1) and miRNAs (pre-miR-23b or pre-miR-27b) were stained with Cleaved-Casp3 antibody or with TUNEL staining kit after hypoxia treatment (24 h) at DIV5. (c) Statistical analysis of the percentage of Cleaved-Casp3-positive neurons or TUNEL-positive neurons to DAPI-stained cells (cell numbers = 700–800, unpaired t -test, $**P<0.01$ and $***P<0.001$). Scale bar represents 100 μ m

staining-positive neurons were significantly reduced in transgenic pups after hypoxia treatment. Therefore, the elevation of the expression of the miR-23a/b and miR-27a/b clusters may suppress the neuronal apoptosis induced by pathological injuries.

Apaf-1 protein levels are extremely low in adult brains, and the expressions of the miR-23-27 clusters are significantly higher in adults than in embryos. To further examine the roles of the miR-23-27 clusters on neuronal apoptosis in adults, it is

needed to knock out or knock down the expression of the miR-23-27 clusters in future studies. However, both miR-23a-27a and miR-23b-27b clusters suppress Apaf-1 expression. Thus, double genome loci should be knocked out if we want to completely knock out the miR-23-27 clusters. The technical difficulty of knocking out each of these miRNAs hinders our ability to perform a loss-of function study. Perhaps, the miRNA sponge technique could be used to construct a functional miRNA knockdown transgenic mouse in

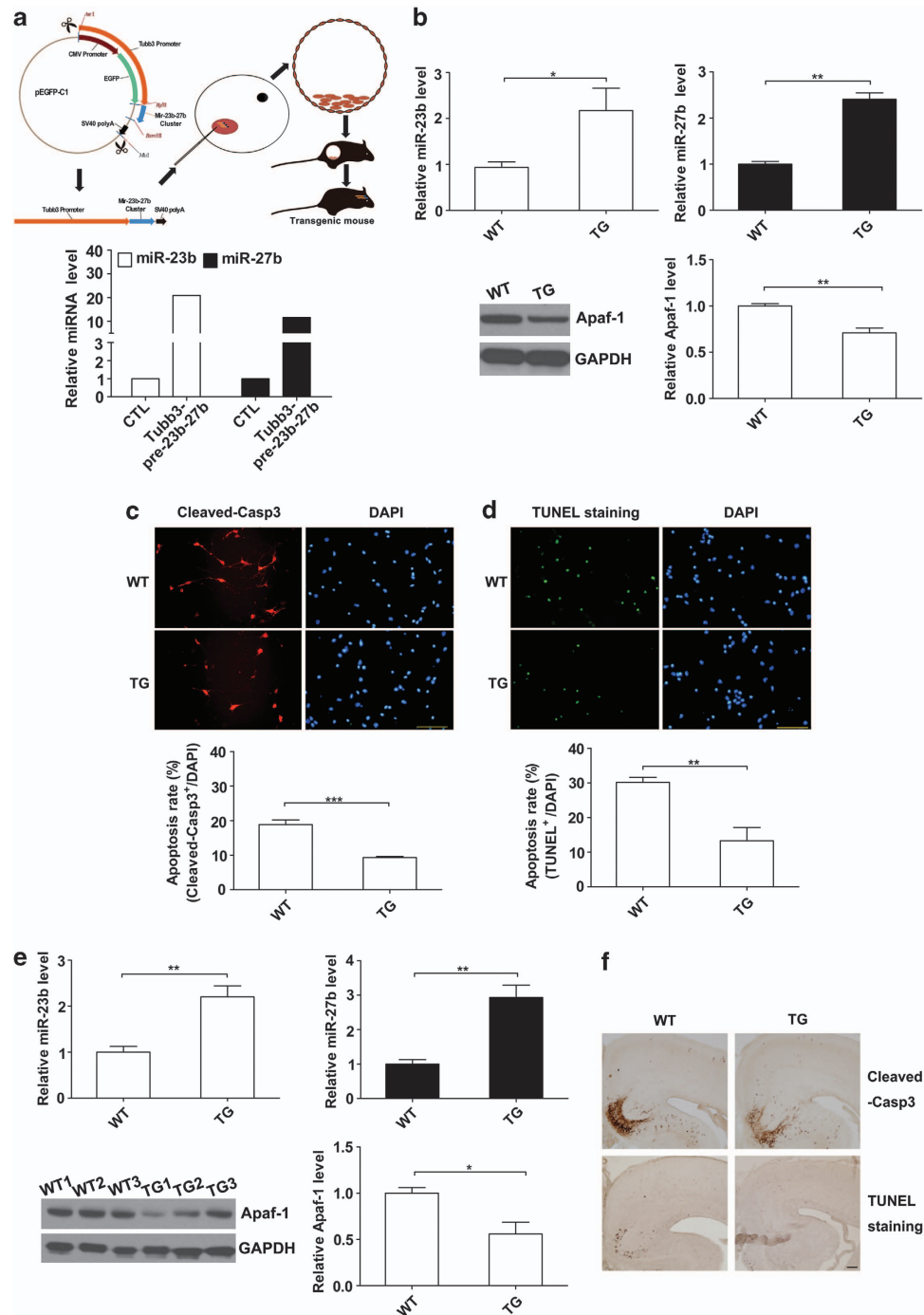


Figure 7 The miR-23b-27b transgenic mice show more resistance to hypoxia-induced apoptosis. (a) A cartoon of generation of the miR-23b-27b cluster transgenic mice. The *Tubb3* gene promoter was employed because of its high expression capability and specificity in neurons in the early embryonic stage. Quantitative RT-PCR detection of miR-23b and miR-27b in primary cortical neurons 24 h after transfection with the constructed plasmid. (b) Quantitative RT-PCR detection of miR-23b-27b (top) and western blot analysis of Apaf-1 protein levels (bottom) in cultured primary cortical neurons from wild-type (WT) mice and transgenic (TG) mice ($n = 3$, unpaired t -test, * $P < 0.05$ and ** $P < 0.01$). (c) Cultured cortical neurons isolated from E15.5 pups were stained with Cleaved-Casp3 antibody after hypoxia treatment (24 h) at DIV5 and counterstained with DAPI. Statistical analysis of the percentage of Cleaved-Casp3-positive neurons to DAPI-stained cells (cell numbers = 400–500, unpaired t -test, *** $P < 0.001$). Scale bar represents 100 μm . (d) Cultured cortical neurons were stained with TUNEL staining kit after hypoxia treatment. Statistical analysis of the percentage of TUNEL-positive neurons to DAPI-stained cells (cell numbers = 400–500, unpaired t -test, ** $P < 0.01$). (e) Quantitative RT-PCR detection of miR-23b-27b (top) and western blot analysis of Apaf-1 protein levels (bottom) in the cerebral cortices from E19.5 mice (TG mice $n = 4$ and WT mice $n = 6$, unpaired t -test, * $P < 0.05$ and ** $P < 0.01$). (f) Coronal sections of WT and transgenic neocortex at E19.5 were stained with Cleaved-Casp3 antibody after 6 h of hypoxia followed by a 6-h recovery or with TUNEL staining kit after a 18-h recovery. Scale bar represents 100 μm

the future.³³ With this miR-23-27 sponge transgenic mouse, the roles of the miR-23-27 clusters in adults could be further explored.

Apaf-1 protein levels were elevated, whereas Apaf-1 mRNA levels did not change significantly after hypoxia (data not shown). Interestingly, miR-23 and miR-27 expression levels were downregulated earlier after hypoxia. These results suggest that hypoxia downregulated the expression of miR-23b and miR-27b, and this downregulation relieved the suppression of Apaf-1 protein. However, the mechanism by which the expression of the miR-23-27 clusters in neurons is regulated is still unknown, and the pathway by which hypoxia downregulates the expression of the miR-23-27 clusters is also unknown. Further studies are needed to explain the mechanism by which the miR-23b-27b cluster is downregulated by hypoxia.

Taken together, our finding suggests a potential molecular mechanism underlying age-dependent differences in which the miR-23-27 clusters normally repress Apaf-1 gene expression in the nervous system during development. In addition, the acute brain injury induced by hypoxia appears to suppress the expression of miR-23-27 clusters and leads to greater neuronal apoptosis. Upregulating the expression of miR-23-27 clusters may help to protect neurons from injury-induced apoptotic cell death during development.

Materials and Methods

Animals and reagents. C57BL/6J mice (from embryos to adults) were employed in the present study. All animals were handled in accordance with the NIH Guidelines for the Care and Use of Laboratory Animals and the protocols were approved by the Animal Care Committee of Nanjing University (Nanjing, China). All of the reagents used in this study were of analytical grade or molecular biology grade.

Cell culture, transfection, and hypoxia treatment

in vitro. HEK293T cells were ordered from the Type Culture Collection of the Chinese Academy of Sciences (Shanghai, China). Dissociated cortical neurons were prepared from E14.5–E15.5 cortices of C57BL/6J mice and cultured in Neurobasal medium (Life Technologies, Grand Island, NY, USA) containing 2% B27 (v/v, Life Technologies), 1 mM L-glutamine, 100 IU/ml penicillin, and 100 µg/ml streptomycin. B27 minus AO (Life Technologies) was substituted for B27 during the exposure of cortical neurons to hypoxia. HEK293T cells were transfected using Lipofectamine 2000 reagent (Invitrogen, Carlsbad, CA, USA), following the manufacturer's manual. Primary cortical neurons were transfected at DIV3 as described previously by An *et al.*³⁴ To induce hypoxia in cultured neurons, anaeroPack bags (Mitsubishi Gas Chemical Company, Inc., MGC, Tokyo, Japan) were employed; cultured neurons at DIV5 were put into the bags, and the entire bags were incubated in a CO₂ incubator for 6, 12, or 24 h.

RNA isolation and quantitative RT-PCR. Total RNA was extracted from tissues and the cultured cells using Trizol reagent (Invitrogen) according to the manufacturer's instructions. For quantitative RT-PCR analysis of mRNA, 1 µg of total RNA was reverse transcribed to cDNA with oligo(dT) and ThermoScript (TaKaRa, Dalian, China). Real-time PCR was performed on an Applied Biosystems 7300 Sequence Detection System (Applied Biosystems, Foster City, CA, USA) using SYBR green dye (Roche, Mannheim, Germany). The sequences of the primers used for gene amplification were as follows: Apaf-1 (forward): 5'-GTTGATGCTGTCATTATGTAGGC-3'; Apaf-1 (reverse): 5'-AGGTAAAAGGG GAAGTATGTGTT-3'; β-actin (forward): 5'-CTGTCCCTGTATGCCTCTG-3'; and β-actin (reverse): 5'-ATGTCACGCACGATTTCC-3'. Quantitative RT-PCR of mature miRNAs was performed using TaqMan miRNA probes (Ambion, Austin, TX, USA) according to the manufacturer's instructions. β-Actin and U6 snRNA were used for normalization in gene and miRNA expression studies, respectively. A relative fold change in expression of the target gene transcript was calculated with the equation $2^{-\Delta\Delta CT}$.

Plasmid construction and luciferase reporter assay. A 507-bp segment of the 3'-UTR of Apaf-1 that contained the presumed miRNAs binding sites was amplified by PCR using mouse cDNA as a template with the following using primer sets: forward, 5'-GGACTAGTCACACTAGACAGGCACTCCACCG-3'; reverse, 5'-CCCAAGCTTGTTCAGCAAGGAAAGGGCCACAA-3' (the *SpeI* and *HindIII* restriction sites were added for cloning). The PCR products were inserted into the p-MIR-report plasmid (Ambion). To test the binding specificity, we mutated the complementary site of miR-23a/b from AATGTGA to TTACACT and the complementary site of miR-27a/b from TACTGTGA to ATGACACT. For luciferase reporter assays, HEK-293T cells were cultured in 24-well plates, and each well was transfected with 0.2 µg of firefly luciferase reporter plasmid, 0.2 µg of β-galactosidase (β-gal) expression vector (Ambion), and 20 pmol of a precursor miRNA oligo using the Lipofectamine 2000 reagent (Invitrogen) according to the manufacturer's instructions. The β-gal vector was used as a transfection control. At 24 h post transfection, the cells were assayed using luciferase assay kits (Promega, Madison, WI, USA). The data depicted are representative of five independent experiments performed on different days.

MiRNA in situ hybridization. For tissue sections, brains of E18 and adult mice were dissected and fixed in 4% paraformaldehyde (PFA) in phosphate-buffered saline (PBS) overnight at 4°C. Next, brains were cryoprotected in 15% sucrose and 30% sucrose in PBS and cut into 20-µm-thick coronal sections on a Leica cryostat after being embedding into an OCT compound. Brain cryostat sections were fixed in 4% PFA, pretreated with proteinase K, and hybridized with digoxigenin (DIG)-labeled Locked Nucleic Acid (LNA) probes (Exiqon, Woburn, MA, USA) in a 50% formamide hybridization mix at 45°C. Slides were then washed with 0.1 × SSC at 50°C. The DIG-labeled probes were detected by alkaline phosphatase (AP)-coupled anti-DIG (1:1000, Roche) followed by color development (substrate: BCIP/NBT, Invitrogen). The following probes were used: a probe for miR-23b (5'-GGTAATCCCTGGCAATGTGAT-3') and a scrambled control probe (5'-GTGTAACACGTCTATACGCCCA-3'). The images were taken by an OLYMPUS IX-71 fluorescence inverted microscope (Olympus, Tokyo, Japan).

RNA dot blot. RNA (2.0 µg) was degenerated and transferred to a nylon membrane according to the standard protocol. The membrane was crosslinked and dried. The membrane was prehybridized in DIG Easy Hyb (Roche) for 30 min at 45°C and hybridized with DIG-labeled LNA probes (Exiqon) in a DIG Easy Hyb at 45°C for 12 h according to the manufacturer's instructions. After an extensive washing, the membrane was incubated with AP-coupled anti-DIG (1:1000, Roche) for 1 h at room temperature and detected with CDP-Star reagent (Roche).

Western blot. Samples of tissues and cultured cells were lysed in RIPA sample buffer and centrifuged at 12000 × g for 10 min at 4°C. The supernatant fraction was collected, and the protein concentration was determined by a BCA assay (Pierce, Rockford, IL, USA). Proteins were fractionized on SDS-polyacrylamide gels and transferred to polyvinylidene difluoride membranes. The membranes were blocked for 1 h, followed by an overnight incubation at 4°C with antibodies. After washes, membranes were incubated at room temperature for 1 h with the appropriate secondary antibody conjugated to horseradish peroxidase and detected with an enhanced chemiluminescence reagent (Cell Signaling Technology Inc., Danvers, MA, USA). The intensity of each band was scanned and quantified using BandScan software (Glyko Inc., Novato, CA, USA). The following antibodies were used: anti-Apaf-1 (rabbit, 1:500, Abcam, ab32372, Cambridge, MA, USA) and anti-cleaved caspase-3 (rabbit, 1:1000, Cell Signaling Technology Inc., 9661).

IHC and immunofluorescence staining. Coronal brain sections, 20-µm-thick, or primary cultured neurons were fixed in 4% PFA, incubated with PBS containing 0.3% hydrogen peroxide for 30 min, and blocked for 1 h at room temperature. Samples were incubated with primary antibodies at 4°C overnight, followed by incubation in a biotinylated secondary antibody for 2 h at room temperature. Antibody detection was amplified with a commercial catalyzed signal amplification kit (VECTASTAIN Elite ABC Kit; Linaris, Wertheim, Germany), according to the manufacturer's instructions. Reactions were visualized with DAB (Sigma, St. Louis, MO, USA). For immunofluorescence staining, incubation of Alexa Fluor 594-conjugated secondary antibody (1:1000, Invitrogen) was performed in a dark room at room temperature. Nuclei were counterstained with DAPI (Sigma) for 5 min and then washed in PBS.

siRNA and Apaf-1 overexpression plasmid. The siRNAs targeting mouse Apaf-1 (5'-GAUGGUCCUUGCAGUUGACAACAU-3', 5'-UAUGUUGUCAACUGCAAGGACCAUC-3') and control siRNA were purchased from Invitrogen. Plasmid overexpressing Apaf-1 (pCMV6-Apaf-1; RC213433) and control plasmid (pCMV6; PS100001) were purchased from OriGene Technologies (Rockville, MD, USA).

Hypoxia treatment *in vivo*. Pregnant C57BL/6J wild-type mice (mated with male miR-23b-27b transgenic mice) were exposed to systemic hypoxia at the late stage of mouse gestation (gestation day 20; i.e., E19.5 for the pup). Mice were kept in continuous hypoxia with an inspired O₂ fraction of 6% for 6 h (gas mixture: 6% O₂, 94% N₂; Hypoxic chambers, Coy Labs, Grass Lake, MI, USA). To enable adjustment to the hypoxic environment, O₂ levels were gradually decreased from an O₂ fraction of 21 to 6% in 2% steps every 10 min, as described previously.³⁵ Controls were kept in the chamber under room air. After the incubation period, neonatal brains were dissected immediately or after a period of recovery (6 or 18 h). Cerebral cortices were isolated, frozen in liquid nitrogen, and stored at -70°C until protein and RNA extraction. For the IHC and TUNEL studies, the mice were allowed to recover after the hypoxia period (6 h for cleaved caspase-3 staining and 18 h for TUNEL staining) before brain tissues were dissected and stained.

TUNEL assay. The brains of embryos were dissected and fixed in 4% PFA. Coronal brain sections were obtained, as described above. TUNEL assays were performed with an *in situ* apoptosis detection kit (KeyGEN BioTECH, Nanjing, China) according to the manufacturer's instructions.

Generation of miR-23b-27b transgenic mice. A schematic diagram of the transgenic construct is shown in Figure 7a. The mouse 3050-bp *Tubb3* promoter was cloned by PCR from C57BL/6J mouse genomic DNA using the following primer sets: forward, 5'-GTTATTAATGTCGACAGGATGAGCTTAAATAG-3'; reverse, 5'-GAAGATCTGCTGACTTCACGCGCTAGAGACGA-3' (the *Asel* and *BglII* restriction sites were added for cloning). The mouse 613-bp miR-23b-27b cluster was cloned by PCR from C57BL/6J mouse genomic DNA using the following primer sets: forward, 5'-GAAGATCTTCTAGAGCTAGCGAATTCCTCTC-3'; reverse, 5'-CGGGATCCGATCGAGATCCTTCGCGGC-3' (the *BglII* and *BamHI* restriction sites were added for cloning). These DNA fragments were subcloned into pEGFP-C1 plasmids (Clontech, Mountain View, CA, USA). The Nanjing Biomedical Research Institute of Nanjing University (NBRI, Nanjing University, China) provided the service to inject the miR-23b-27b transgenic construct into the pronuclei of C57BL/6J zygotes and implanted into pseudopregnant recipient females. Mice were genotyped by PCR using primers for miR-23b-27b cluster transgenic mouse (forward 5'-ATCTCGGTGCCGGTCTGATGCT-3'; reverse 5'-GTCCGATTAGTGGATGTTTCTGTGG-3').

Statistical analysis. Data are presented as mean ± S.E.M. of at least three independent experiments. Direct comparisons were made using Student's *t*-tests and multiple group comparisons were made using one-way analyses of variance (ANOVA). Statistical significance was defined as $P < 0.05$, 0.01, or 0.001 (indicated as *, **, or ***, respectively). The *P*-values of ≥ 0.05 were considered not significant (indicated as NS). Prism software 5.0 (GraphPad, Inc., La Jolla, CA, USA) was used for data analyses.

Conflict of Interest

The authors declare no conflict of interest.

Acknowledgements. This work was supported by grants from the National Natural Science Foundation of China (31100777 and 81170309 to Qipeng Zhang; 31000478 to Liang Li; 30988003 and 30871019 to Ke Zen; and 90608010 to Chen-Yu Zhang).

Author contributions

Qun Chen, Qipeng Zhang, Jie Xu, Hanqin Li, Liang Li, Susu Mao, and Fan Zhang planned and performed the experiments; Qun Chen and Qipeng Zhang analyzed the data and wrote the manuscript; Chenyu Zhang, Ke Zen, and Qipeng Zhang designed the experiments and revised the manuscript.

1. Nijhawan D, Honarpour N, Wang X. Apoptosis in neural development and disease. *Annu Rev Neurosci* 2000; **23**: 73–87.
2. Kuida K, Zheng TS, Na S, Kuan C, Yang D, Karasuyama H *et al*. Decreased apoptosis in the brain and premature lethality in CPP32-deficient mice. *Nature* 1996; **384**: 368–372.
3. Hakem R, Hakem A, Duncan GS, Henderson JT, Woo M, Soengas MS *et al*. Differential requirement for caspase 9 in apoptotic pathways *in vivo*. *Cell* 1998; **94**: 339–352.
4. Yoshida H, Kong YY, Yoshida R, Elia AJ, Hakem A, Hakem R *et al*. Apaf1 is required for mitochondrial pathways of apoptosis and brain development. *Cell* 1998; **94**: 739–750.
5. Thompson CB. Apoptosis in the pathogenesis and treatment of disease. *Science* 1995; **267**: 1456–1462.
6. Volpe JJ. Perinatal brain injury: from pathogenesis to neuroprotection. *Ment Retard Dev Disabil Res Rev* 2001; **7**: 56–64.
7. McLean C, Ferriero D. Mechanisms of hypoxic-ischemic injury in the term infant. *Semin Perinatol* 2004; **28**: 425–432.
8. Hu BR, Liu CL, Ouyang Y, Blomgren K, Siesjo BK. Involvement of caspase-3 in cell death after hypoxia-ischemia declines during brain maturation. *J Cereb Blood Flow Metab* 2000; **20**: 1294–1300.
9. Puleria MR, Adams LM, Liu H, Santos DG, Nishimura RN, Yang F *et al*. Apoptosis in a neonatal rat model of cerebral hypoxia-ischemia. *Stroke* 1998; **29**: 2622–2630.
10. Sidhu RS, Tuor UI, Del Bigio MR. Nuclear condensation and fragmentation following cerebral hypoxia-ischemia occurs more frequently in immature than older rats. *Neurosci Lett* 1997; **223**: 129–132.
11. Yakovlev AG, Ota K, Wang G, Movsesyan V, Bao WL, Yoshihara K *et al*. Differential expression of apoptotic protease-activating factor-1 and caspase-3 genes and susceptibility to apoptosis during brain development and after traumatic brain injury. *J Neurosci* 2001; **21**: 7439–7446.
12. Li P, Nijhawan D, Budihardjo I, Srinivasula SM, Ahmad M, Alnemri ES *et al*. Cytochrome c and dATP-dependent formation of Apaf-1/caspase-9 complex initiates an apoptotic protease cascade. *Cell* 1997; **91**: 479–489.
13. Ceconi F, Alvarez-Bolado G, Meyer BI, Roth KA, Gruss P. Apaf1 (CED-4 homolog) regulates programmed cell death in mammalian development. *Cell* 1998; **94**: 727–737.
14. Johnson CE, Huang YY, Parrish AB, Smith MI, Vaughn AE, Zhang Q *et al*. Differential Apaf-1 levels allow cytochrome c to induce apoptosis in brain tumors but not in normal neural tissues. *Proc Natl Acad Sci USA* 2007; **104**: 20820–20825.
15. Baek D, Villen J, Shin C, Camargo FD, Gygi SP, Bartel DP. The impact of microRNAs on protein output. *Nature* 2008; **455**: 64–71.
16. Bartel DP. MicroRNAs: target recognition and regulatory functions. *Cell* 2009; **136**: 215–233.
17. He L, Hannon GJ. MicroRNAs: small RNAs with a big role in gene regulation. *Nat Rev Genet* 2004; **5**: 522–531.
18. Kloosterman WP, Plasterk RH. The diverse functions of microRNAs in animal development and disease. *Dev Cell* 2006; **11**: 441–450.
19. Miska EA, Alvarez-Saavedra E, Townsend M, Yoshii A, Sestan N, Rakic P *et al*. Microarray analysis of microRNA expression in the developing mammalian brain. *Genome Biol* 2004; **5**: R68.
20. Sempere LF, Freemantle S, Pitha-Rowe I, Moss E, Dmitrovsky E, Ambros V. Expression profiling of mammalian microRNAs uncovers a subset of brain-expressed microRNAs with possible roles in murine and human neuronal differentiation. *Genome Biol* 2004; **5**: R13.
21. Juhila J, Sipilä T, Icaý K, Nicorici D, Ellonen P, Kallio A *et al*. MicroRNA expression profiling reveals miRNA families regulating specific biological pathways in mouse frontal cortex and hippocampus. *PLoS One* 2011; **6**: e21495.
22. Li X, Jin P. Roles of small regulatory RNAs in determining neuronal identity. *Nat Rev Neurosci* 2010; **11**: 329–338.
23. Sun AX, Crabtree GR, Yoo AS. MicroRNAs: regulators of neuronal fate. *Curr Opin Cell Biol* 2013; **25**: 215–221.
24. Zhang L, Dong LY, Li YJ, Hong Z, Wei WS. miR-21 represses FasL in microglia and protects against microglia-mediated neuronal cell death following hypoxia/ischemia. *Glia* 2012; **60**: 1888–1895.
25. Doepfner TR, Doehring M, Bretschneider E, Zechariah A, Kaltwasser B, Muller B *et al*. MicroRNA-124 protects against focal cerebral ischemia via mechanisms involving Usp14-dependent REST degradation. *Acta Neuropathol* 2013; **126**: 251–265.
26. Rehmsmeier M, Steffen P, Hochsmann M, Giegerich R. Fast and effective prediction of microRNA/target duplexes. *RNA* 2004; **10**: 1507–1517.
27. Haydar TF, Kuan CY, Flavell RA, Rakic P. The role of cell death in regulating the size and shape of the mammalian forebrain. *Cereb Cortex* 1999; **9**: 621–626.
28. Northington FJ, Chavez-Valdez R, Martin LJ. Neuronal cell death in neonatal hypoxia-ischemia. *Ann Neurol* 2011; **69**: 743–758.
29. Liu L, Geisert EE, Frankfurter A, Spano AJ, Jiang CX, Yue J *et al*. A transgenic mouse class-III beta tubulin reporter using yellow fluorescent protein. *Genesis* 2007; **45**: 560–569.
30. Lian S, Shi R, Bai T, Liu Y, Miao W, Wang H *et al*. Anti-miRNA-23a oligonucleotide suppresses glioma cells growth by targeting apoptotic protease activating factor-1. *Curr Pharm Des* 2013; **19**: 6382–6389.

31. Betel D, Koppal A, Agius P, Sander C, Leslie C. Comprehensive modeling of microRNA targets predicts functional non-conserved and non-canonical sites. *Genome Biol* 2010; **11**: R90.
32. Gao Y, Liang W, Hu X, Zhang W, Stetler RA, Vosler P *et al*. Neuroprotection against hypoxic-ischemic brain injury by inhibiting the apoptotic protease activating factor-1 pathway. *Stroke* 2009; **41**: 166–172.
33. Ebert MS, Neilson JR, Sharp PA. MicroRNA sponges: competitive inhibitors of small RNAs in mammalian cells. *Nat Methods* 2007; **4**: 721–726.
34. An JJ, Gharami K, Liao GY, Woo NH, Lau AG, Vanevski F *et al*. Distinct role of long 3' UTR BDNF mRNA in spine morphology and synaptic plasticity in hippocampal neurons. *Cell* 2008; **134**: 175–187.
35. Trollmann R, Strasser K, Keller S, Antoniou X, Grenacher B, Ogunshola OO *et al*. Placental HIFs as markers of cerebral hypoxic distress in fetal mice. *Am J Physiol Regul Integr Comp Physiol* 2008; **295**: R1973–R1981.



Cell Death and Disease is an open-access journal published by *Nature Publishing Group*. This work is licensed under a Creative Commons Attribution-NonCommercial-NoDerivs 3.0 Unported License. To view a copy of this license, visit <http://creativecommons.org/licenses/by-nc-nd/3.0/>

Supplementary Information accompanies this paper on Cell Death and Disease website (<http://www.nature.com/cddis>)